



Contents lists available at ScienceDirect

Fungal Genetics and Biology

journal homepage: www.elsevier.com/locate/yfgbi

Aspergillus nidulans UDP-galactopyranose mutase, encoded by *ugmA* plays key roles in colony growth, hyphal morphogenesis, and conidiation

Amira M. El-Ganiny^a, David A.R. Sanders^b, Susan G.W. Kaminskyj^{a,*}^a Department of Biology, University of Saskatchewan, 112 Science Place, Saskatoon, SK, Canada S7N 5E2^b Department of Chemistry, University of Saskatchewan, 110 Science Place, Saskatoon, SK, Canada S7N 5C9

ARTICLE INFO

Article history:

Received 13 February 2008

Accepted 17 September 2008

Available online xxxx

Keywords:

Aspergillus nidulans

Cell wall

Galactofuranose

Hyphal morphogenesis

Conidiation

UDP-galactopyranose mutase

ABSTRACT

Growing resistance to current anti-fungal drugs is spurring investigation of new targets, including those in fungal wall metabolism. Galactofuranose (Gal_f) is found in the cell walls of many fungi including *Aspergillus fumigatus*, which is currently the most prevalent opportunistic fungal pathogen in developed countries, and *A. nidulans*, a closely-related, tractable model system. UDP-galactopyranose mutase (UGM) converts UDP-galactopyranose into UDP-Gal_f prior to incorporation into the fungal wall. We deleted the single-copy UGM sequence (AN3112.4, which we call *ugmA*) from an *A. nidulans nkuAΔ* strain, creating *ugmAΔ*. Haploid *ugmAΔ* strains were able to complete their asexual life cycle, showing that *ugmA* is not essential. However, *ugmAΔ* strains had compact colonial growth, which was associated with substantially delayed and abnormal conidiation. Compared to a wildtype morphology strain, *ugmAΔ* strains had aberrant hyphal morphology, producing wide, uneven, highly-branched hyphae, with thick, relatively electron-dense walls as visualized by transmission electron microscopy. These effects were partially remediated by growth on high osmolarity medium, or on medium containing 10 μg/mL Calcofluor, consistent with Gal_f being important in cell wall structure and/or function.

© 2008 Elsevier Inc. All rights reserved.

1. Introduction

In the last decades there has been an increase in the incidence of fungal infections due to immunocompromising conditions such as AIDS and organ transplantation, and perhaps also to overuse of broad-spectrum antibiotics (Loffler and Stevens, 2003; García-Ruiz et al., 2004). Mortality in patients with systemic fungal infections is high even with aggressive therapy (Randhawa and Sharma, 2004). *Aspergillus fumigatus* is the most common opportunistic fungal pathogen in industrialized countries, due to their relatively large populations at risk (Arathoon, 2001). *A. fumigatus* is common in the environment (where it contributes to recycling), has air-dispersed spores that are readily inhaled, and has a growth optimum near 37 °C.

Treatment of fungal infections is limited by problems of drug safety, effectiveness and fungal resistance (Cowen, 2008). Polyene antifungals lack target specificity and have a high toxicity to humans; azoles are fungistatic, not fungicidal; echinocandins have a narrow spectrum of activity; and apart from polyenes, there is

emerging antifungal drug resistance (Carrillo-Munoz et al., 2006; Chamilos and Kontoyiannis, 2005). An anti-fungal drug target should be found in a broad spectrum of fungal pathogens, be important for infectivity, and not be found in humans. Fungal cell wall components, including chitin, β1–3 glucans, and galactofuranose (Notermans et al., 1998; Leitao et al., 2003) are obvious drug targets (Tawara et al., 2000; Pederson and Turco, 2003; Schmalhorst et al., 2008).

Genetic and biochemical studies of Gal_f biosynthesis in prokaryotes show that UDP-Gal_f (the five-membered ring form, Fig. 1) is formed from UDP-Galp (the six-membered ring form) by UDP-galactopyranose mutase (UGM) (Nassau et al., 1996; Weston et al., 1998). UDP-Gal_f is the precursor to Gal_f residues found in the cell walls of many microorganisms. The gene encoding UGM has been identified in prokaryotes (Stevenson et al., 1996; Nassau et al., 1996; Koplín et al., 1997; Pan et al., 2001) and its crystal structure has been solved (Sanders et al., 2001).

Galactofuranose (Gal_f) is an essential component of the bacterial cell wall (Whitfield et al., 1991; Nassau et al., 1996; Pan et al., 2001), and is important or essential for pathogenicity of *Leishmania major* (Spath et al., 2000; Kleczka et al., 2007), which causes leishmaniasis. Beta-linked Gal_f chains are the immunodominant epitope in *Aspergillus* spp. (Bennett et al., 1984; Latgé et al., 1994; Leitao et al., 2003). In *A. niger*, *ugmA* contributes to cell wall integrity (Damveld et al., 2008). In *Aspergillus fumigatus*, the *ugmA*

Abbreviations: Gal_f, Galactofuranose; SEM, scanning electron microscopy; TEM, transmission electron microscopy; UGM, UDP-galactopyranose mutase; *ugmA*, *Aspergillus nidulans* UGM-encoding gene; *ugmAΔ*, *ugmA* deletion.

* Corresponding author. Fax: +1 306 966 4461.

E-mail address: Susan.Kaminskyj@usask.ca (S.G.W. Kaminskyj).

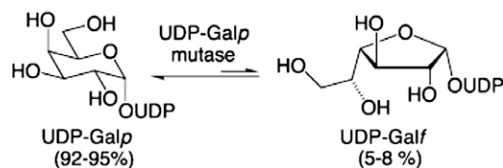


Fig. 1. Interconversion of UDP-galactopyranose (UDP-Galp) and UDP-galactofuranose (UDP-Galf) by UDP galactopyranose mutase. The equilibrium of this reaction is heavily in favour of UDP-Galp.

homologue *glfA* contributes to wildtype wall structure (Schmalhorst et al., 2008). Galf has been shown to be attached to linear mannan chains in the *A. fumigatus* cell wall, which are GPI-anchored to the cell membrane (Costachel et al., 2005; Schmalhorst et al., 2008). *A. fumigatus* and *A. nidulans* hyphal walls have similar galactose content (Guest and Momany, 2000). The Galf monoclonal antibody EBA2 has been used for diagnosis of aspergillosis and to monitor therapy effectiveness (Stynen et al., 1992; Wallis et al., 2001; Maertens et al., 2007).

Beverly et al. (2005) identified eukaryotic UGM genes in protozoa (*L. major* and *Trypanosoma cruzi*) and the fungus (*Cryptococcus neoformans*). Beverly et al. (2005) found that eukaryote UGM amino acid sequences are closely related to each other but distantly related to prokaryote UGMs. *A. fumigatus* and *L. major* UGM shared 51% sequence identity, but were less than 20% identical to their prokaryotic orthologues, with the region of identity/similarity confined to the catalytic site (Bakker et al., 2005). Eukaryote UGMs have four major insertions, which are thought to form loops that are important for protein regulation and interaction.

BLAST analysis with default parameters using *A. fumigatus* UGM (Afu3g12690, named *AfglfA* by Schmalhorst et al. (2008)) at <http://www.broad.mit.edu/annotation/fungi/aspergillus/> showed a strong sequence alignment (98% identity) to one locus in *A. nidulans*, AN3112.4, which we named *ugmA*. We are using *A. nidulans* as a safe and experimentally tractable system for studying UGM function *in vivo*, in parallel with crystallization studies of *A. fumigatus glfA*. This study focuses on the effects of *UgmA* deletion in *A. nidulans*. We found that *ugmA* was not essential, but its deletion resulted in compact colonial growth, reduced sporulation, and hyphal morphological abnormalities, all of which can be attributed to wall defects.

2. Materials and methods

Biological materials and primers are given in Table 1. Chemicals were reagent grade and were purchased from VWR (<http://www.vwrcanlab.ca>) or Sigma (<http://www.sigmaaldrich.com>) unless stated otherwise. Vinoflow was purchased from Gusmer Enterprises (<http://www.thewinelab.com>). Water was 18 M Ω deionized, and sterilized as appropriate. *Aspergillus nidulans* strains were grown in complete media CM with nutritional supplements as required (Kaminskyj, 2001).

Statistical analysis used Statview SE+Graphics v1.02. Values are presented as means \pm standard error of the mean. Images were prepared with Adobe Photoshop 7.0.

2.1. Gene knockout

Aspergillus nidulans strain A1149 was used for AN3112 (*ugmA*) gene deletion, following the procedures described in Nayak et al. (2006) and Szewczyk et al. (2007), with *A. fumigatus pyrG* as the selectable marker (Fig. 2A–F). Experiments using *A. fumigatus pyrG* selection (not shown) gave comparable results. A1149 was also transformed to pyrimidine prototrophy as described in Yang et al. (2008), creating AAE1, a wildtype phenotype *pyrG*⁺, *nkuA* Δ

Table 1
Biological materials used in this study

<i>Aspergillus nidulans</i>	
A1149 ^a	<i>pyrG89</i> ; <i>pyroA4</i> ; <i>nkuA::argB</i>
AAE1 ^b	<i>pyrG89::N. crassa pyr4⁺</i> ; <i>pyroA4</i> ; <i>nkuA::argB</i>
AAE2 (<i>ugmA</i> Δ) ^b	AN3112:: <i>AfpyrG</i> ; <i>pyrG89</i> ; <i>pyroA4</i> ; <i>nkuA::argB</i>
AAE3 (<i>ugmA</i> Δ :: <i>AfglfA</i>) ^b	AN3112:: <i>AfpyrG</i> ; <i>pyrG89</i> ; <i>pyroA4</i> ; <i>nkuA::argB</i> ; <i>AfglfA</i>
AOZ1 ^b	<i>swoA1</i> ; <i>wA3</i> , <i>GFP-tubA</i>
Plasmids	
ARp1 ^c	AMA1, <i>Neurospora crassa pyr4⁺</i> , <i>amp</i> ^R
pAO81 ^a	S-TAG, <i>A. fumigatus pyrG</i> , <i>kan</i> ^R
pET22 ^d	<i>A. fumigatus glfA</i> , <i>amp</i> ^R
Primers 5' \rightarrow 3' ^b	
P1	GACTCTTGAGATTTGCTTGGGTCTC
P2	CCTGGAGCATTCCTTGCTCTG
P3	AATTGCGACTTGGACGACATAGAAGAGAGCGAAGCTGCAG
P4	GAGTATGCGGCAAGTCATGAAATAAACTCTTCTGCGGTGG
P5	CTGTTTGGCCGCTAATAGC
P6	GTGTTTACCAAGAATATGTTTCATCGA
P8	CACATCCGACTGCACTTCC
P21	ATGCTTAGTCTAGCTCGCAAGAC
P23	CTGGCCTTATTCTTAGCAAA
AfpyrGF	ATGTCGTCCAAGTCGCAATT
AfpyrGR	TCATGACTTGCCTGCACTC
AfugmAF	CCCTCCAGCTCCGTCGAC
AfugmAR	CTGGCCTTGCCTTGGC
nkuAF	CCCGTCCGCTCTGCAG
nkuAR	AACTTCGTCTCAAGTAACTCCTCCAC

^a <http://www.fgsc.net>.

^b This study.

^c Shi et al. (2004).

^d Bakker et al. (2005).

strain used for phenotype comparison. Following transformation, putative *ugmA* Δ colonies were able to conidiate on selective media. These conidia were inoculated onto selective and non-selective media to assess whether *ugmA* was essential (Osmani et al., 2006). Spores were also grown on selective media to examine hyphal and colony morphology under different growth conditions, and to generate mycelium for genomic DNA extraction, as described in Yang et al. (2008). PCR comparing A1149 genomic DNA with that from three *ugmA* Δ deletion strains used the primers described in Fig. 2 and Table 1.

2.2. Microscopical methods

2.2.1. Confocal microscopy

Aspergillus nidulans wildtype and *ugmA* Δ strains were grown at 28 °C, then samples were fixed and stained with Calcofluor to visualize walls and Hoechst 33258 to visualize nuclei, as described in Kaminskyj and Hamer (1998). Confocal imaging used a Zeiss META510 confocal microscope with a 63 \times , 1.2 N.A. multi-immersion objective, a 405 nm diode at 20% power, and a 420–480 nm emission filter. Fluorescence and transmitted light images were collected simultaneously.

For morphometry, hyphal width was measured at septa (50 per strain), and basal cell length was measured between adjacent septa (50 per strain) as previously described in Kaminskyj and Hamer (1998). Total hyphal length per germling was measured using Zeiss LSM software, by adding the lengths of all branches (30 germlings per strain). The number of tips per germling was counted.

For immunofluorescence microscopy, samples were prepared as described in Kaminskyj and Heath (1995). EBA2 monoclonal antibody originally raised against *A. fumigatus* galactomannan, which contains Galf (Wallis et al., 2001), was eluted from a BioRad Platelia ELISA kit using TBS, and concentrated with a 10 kDa Microcon centrifugal concentration column (Millipore). EBA2 binding was localized using FITC-conjugated goat-anti-rat IgG (Sigma) that had been affinity purified against lyophilized *ugmA* Δ mycelium as described

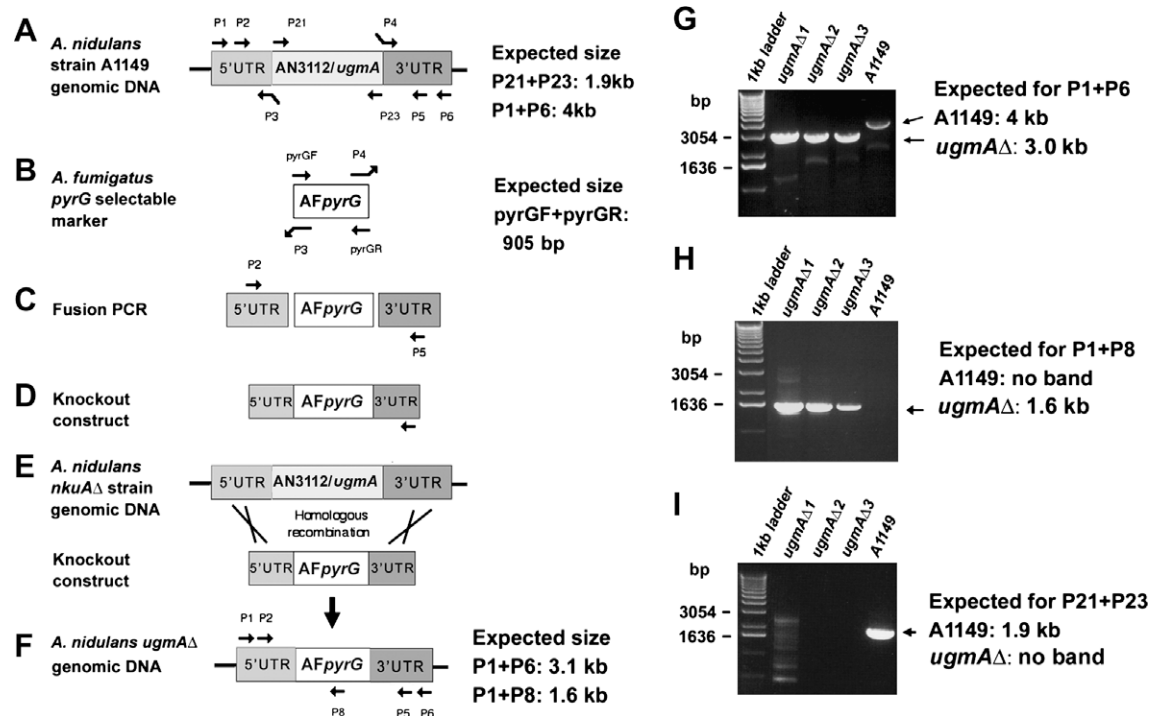


Fig. 2. Strategy for and results of deleting *Aspergillus nidulans* UDP-galactopyranose mutase (*ugmA*) to create *ugmAΔ* strains. (A–F) Deletion strategy. The 5' and 3' regions (5'UTR and 3'UTR, respectively) flanking AN3112 were amplified using P1 + P3 and P4 + P6, respectively, from strain A1149 (*nkuAΔ*, *pyrG89*) genomic DNA template. Primer sequences are in Table 1. P3 and P4 are bridging primers between the flanking regions and the selectable marker. (B) The selectable marker, *A. fumigatus pyrG*, was amplified from plasmid A081 with *pyrGF* and *pyrGR*. (C) Fusion PCR (semi-nested, with P2 + P5) using mixed template (5'UTR, AF*pyrG*, 3'UTR), with complementary ends generated the bridging primers P3 and P4, created (D) the linear AN3112 knockout construct with AN3112 flanking regions. (E) A1149 protoplasts were transformed with the knockout construct. Homologous recombination between the flanking regions replaced AN3112 with AF*pyrG*, creating *ugmAΔ*. The flanking regions were not altered by the homologous recombination, so primer sites remain intact. (F) Predicted *ugmAΔ* genomic DNA. (G–I) PCR comparisons of genomic template from A1149 and *ugmAΔ* strains. (G) Using primers P1 + P6, to amplify *ugmA* plus flanking regions. (H) Using primers P1 + P8, to demonstrate that AF*pyrG* had integrated at the *ugmA* locus. (I) Using primers P21 + P23, to demonstrate the presence of *ugmA* in A1149, and its absence from the *ugmAΔ* strains.

in Kaminskyj and Heath (1995). Confocal imaging used 488 nm excitation, 5–10% power from an argon multispectral laser operated at 5.9 A, with emission controlled by a BP505-530 filter.

2.2.2. Electron microscopy

For scanning electron microscopy (SEM), AAE1 and *ugmAΔ* strains were grown on dialysis tubing overlying selective media for 3 d at 28 °C. Isolated colonies were fixed at 100% relative humidity over 4% aqueous OsO₄ for 2 h, frozen to –80 °C, and lyophilized overnight. Samples were mounted on SEM stubs, gold sputter coated for 6 min, and examined with scanning electron microscope JEOL model JSM840A. The accelerating voltage was 20 kV. The beam current for sample examination was 1.5 nA, and for image acquisition was 50 pA.

For transmission electron microscopy (TEM), AAE1 and *ugmAΔ* strains were grown on dialysis tubing overlying selective media (CM, CM + 1 molar sucrose, or CM + 10 μg/mL Calcofluor) for 16 h at 28 °C. Samples were prepared and imaged as described in Kaminskyj (2000).

3. Results

3.1. UDP-galactopyranose mutase deletion

To test whether *ugmA* was essential, we deleted the AN3112.4 coding sequence in the *nkuAΔ* strain A1149 (Fig. 2A–F). The knockout construct was generated using fusion PCR: the selectable marker *A. fumigatus pyrG* was flanked by predicted 5' and 3' untranslated regions for AN3112. The deletion cassette was transformed into A1149 protoplasts as described in Nayak et al. (2006)

and Szweczyk et al. (2007). Transformants were selected on CM lacking pyrimidines, containing 1 M sucrose as osmoticum. Conidia produced by these primary transformants were able to germinate and formed sporulating colonies when streaked on growth medium lacking exogenous pyrimidines, indicating that *A. nidulans ugmA* is not essential.

Ectopic integration of the knockout construct could potentially have contributed to the *ugmAΔ* phenotype. Morphometric characterization of three randomly chosen putative *ugmAΔ* phenotype colonies are given in Table 2. Deletion experiments using *A. fumigatus pyrA* as a selectable marker (not shown) gave comparable results regarding the phenotype of colonies produced by conidia from primary transformants. We interpret a high level of phenotype consistency at the colony and cellular level between multiple transformants from independent experiments, as being evidence of lack interference from ectopic integrants. Additional confirmatory studies are presented below.

Genomic DNA was extracted from A1149 and *ugmAΔ* strains, and used as template for PCR to test for the presence and location of AN3112 and AF*pyrG*. AN3112 is predicted to be 1.9 kb, and AF*pyrG* is predicted to be 0.9 kb. The 5' and 3' flanking regions were 1 kb and 1.1 kb respectively. PCR using P1 and P6 (to span AN3112 plus the 5' and 3' flanking regions) amplified a ~4 kb band from the A1149 parental strain, and a ~3 kb band with *ugmAΔ* strains (Fig. 2G) consistent with replacement of AN3112 with AF*pyrG*. PCR using P1 and P8 (targeted to a flanking region and the middle of AF*pyrG*), produced bands of the 1.6 kb in *ugmAΔ* strains, and did not amplify a band for A1149 (Fig. 2H). PCR using P21 and P23 (designed to amplify *ugmA*) gave no band with any of the *ugmAΔ* strains, and 1.9 kb band with A1149 (Fig. 2I). Additional stud-

Table 2
Morphometric comparison^a of near-isogenic wildtype morphology (AAE1) and UDP-galactopyranose mutase deletion (*ugmAΔ*) strains^{b,c}

A. Growth on CM	AAE1	<i>ugmAΔ1</i>	<i>ugmAΔ2</i>	<i>ugmAΔ3</i>
Hyphal width (μm)	2.7 ± 0.4 ^d	3.6 ± 0.6 ^e	3.3 ± 0.6 ^f	3.6 ± 0.7 ^e
Basal cell length (μm)	26.9 ± 1.2 ^d	14.9 ± 0.7 ^e	19.5 ± 0.9 ^f	15.3 ± 0.6 ^e
Total colony length (μm)	252 ± 25.7 ^d	317 ± 27.3 ^d	378 ± 79.5 ^d	348 ± 25.0 ^d
Total tips per colony	2.4 ± 0.2 ^c	7.6 ± 0.5 ^d	8.3 ± 1.4 ^d	8.2 ± 0.4 ^d
Hyphal growth index (μm hypha/tip)	105	42	46	42
Wall thickness (nm)	54.0 ± 2.4 ^d	204 ± 10.5 ^f	n/a	n/a
B. Growth on amended CM	CM + 1 M sucrose	CM + 10 μg/mL Calcofluor	CM + 10 μg/mL Calcofluor	CM + 10 μg/mL Calcofluor
	AAE1	AAE2	AAE1	AAE2
Hyphal width (μm)	2.4 ± 0.1 ^d	3.1 ± 0.1 ^f	2.6 ± 0.0 ^d	3.1 ± 0.0 ^f
Basal cell length (μm)	26.1 ± 1.4 ^d	15.3 ± 0.7 ^e	20.8 ± 1.1 ^f	21.8 ± 1.5 ^f
Total colony length (μm)	206 ± 13.6 ^e	140 ± 10.4 ^f	209 ± 31.6 ^e	244 ± 20.9 ^d
Total tips per colony	2.8 ± 0.2 ^d	4.1 ± 0.2 ^e	2.7 ± 0.2 ^d	7.2 ± 0.5 ^f
Hyphal growth index (μm hypha/tip)	73	32	77	34
Wall thickness (nm)	n/a	66.0 ± 3.5 ^{de}	n/a	77.8 ± 3.8 ^e

^a Measurements are expressed as means ± standard error, for 50 hyphae (width and basal cell length), 30 colonies (total colony length and total tips per colony), and 10 transmission electron micrograph near-median sections. n/a, not assessed.

^b Strains were grown for 14 h at 28 °C on dialysis tubing overlying agar-solidified medium. See Section 2 for details. AAE2 is *ugmAΔ1*.

^c For each measurement type, values followed by different letters (d–f) are significantly different ($P < 0.05$; ANOVA). Summary statistics: hyphal width ($P = 0.0001$; $F = 54.314$), basal cell length ($P = 0.0001$; $F = 38.772$); total colony length ($P = 0.082$; $F = 2.299$); tips per colony ($P = 0.0001$; $F = 27.115$).

ies re genetic segregation following mating, and complementation of the *ugmAΔ* defect with the *A. fumigatus* homologue are presented below. Three knockout strains, *ugmAΔ1*, *ugmAΔ2*, and *ugmAΔ3*, gave comparable results in all studies. We designated *ugmAΔ1* as AAE2.

Protoplasts were generated from *A. nidulans* AAE2 germlings, transformed with pET22b containing *AfglfA* (which encodes functional *A. fumigatus* UGM: Bakker et al., 2005), and incubated at 37 °C for 3 d. The following data are presented in Supplemental Fig. 1. In addition to many *ugmAΔ* phenotype colonies that showed compact colony growth and limited sporulation, a putative *ugmAΔ::AfglfA* colony was generated that had wildtype growth and abundant conidiation (arrow in Supplemental Fig. 1a). We named this strain AAE3. PCR of AAE3 genomic DNA using primers designed to amplify *AfglfA* showed a band comparable in size to the pET22b control (Supplemental Fig. 1b). Light microscopy of AAE3 revealed wildtype hyphal morphology (Supplemental Fig. 1c), morphometry (Supplemental Fig. 1d), and nuclear distribution unlike AAE2 (Fig. 4A, and Table 2). Young AAE3 conidiophores had abundant metulae and synchronous phialide development (Supplemental Fig. 1c) unlike AAE2 (Fig. 3H).

AAE2 was mated to AOZ1 to determine whether the *ugmAΔ* defect segregated independently, and to create additional strains for future studies (Supplemental Fig. 2). Independent assortment of the *ugmAΔ* phenotype following mating is evidence that the *ugmAΔ* knockout construct underwent homologous rather than ectopic integration. AAE2 mating efficiency is poor: matings with at least three other *A. nidulans* strains were not successful. Cleistothecium maturation was delayed (no outcrossed cleistothecia containing viable spores were isolated until three months), consistent with the suggestion by Adams et al. (1998) that mutations affecting conidiation also compromise sexual development. Both AOZ1 and AAE2 have reduced conidiation (Supplemental Fig. 2a). AOZ1 contains *swaA1*, which can be complemented by a protein *O*-mannosyl transferase (Shaw and Momany, 2002). Amongst 140 progeny from this cross were 43 with wildtype colony growth and sporulation, and equal numbers of green- and white-spored strains, consistent with independent assortment of *ugmAΔ* and *swaA*. As expected, there were also [*ugmAΔ*, *swaA1*] progeny, with severe growth defects at permissive conditions (e.g. arrowheads in Supplemental Fig. 2a).

Genomic DNA was prepared from six randomly selected progeny that showed the *ugmAΔ* phenotype under the growth condi-

tions shown in Supplemental Fig. 2a. PCR with primers *nkuAF* and *nkuAR*, expected to amplify a band of 1981 bp in *nkuA+* strains, amplified this band in three of these *ugmAΔ* progeny, as well as in wildtype strain A28 (Supplemental Fig. 2b). This is evidence that *ugmA* segregates independently of *nkuA*.

The phenotype consistency for multiple strains from independent knockout experiments using *pyrG* and *pyrA* as selectable markers; rescue of the *ugmAΔ* phenotype by *AfglfA*; and independent segregation of *ugmA* with *nkuA* and *swaA* is strong evidence that the AAE2 phenotype discussed below is due to the deletion of *ugmA*, and that *ugmA* encodes *A. nidulans* UGM.

3.2. Colony growth and sporulation

To characterize the effect of *ugmAΔ* on colony growth, AAE1 and AAE2 strains were grown for 3 d on CM lacking exogenous pyrimidines. AAE1 colonies had a wildtype phenotype, with a broad fringe of submerged hyphae extending into the growth medium (arrows in Fig. 3A), whereas AAE2 colonies had a compact colonial morphology with little penetration of the medium. The AAE2 colonies also had reduced sporulation: the centres of AAE1 colonies had strong green pigmentation (Fig. 3A) whereas AAE2 colonies were pale (Fig. 3B). After 3 d growth at 28 °C, isolated AAE1 colonies were about 50% larger in diameter than those of AAE2, 6.0 ± 0.8 mm vs 4.4 ± 0.6 mm, respectively, even without considering the submerged hyphae at the AAE1 colony margins (arrows in Fig. 3A). Viewed from above at 50×, the AAE1 colonies were sporulating abundantly at 3 d (Fig. 3C), with closely spaced conidiophores bearing pigmented conidia, whereas AAE2 conidiophores that produced pigmented spores were widely separated (e.g., arrows in Fig. 3D).

The number of spores produced per colony was estimated for AAE1 and AAE2 strains. After 3 d, individual AAE1 colonies had produced an average of $1.0 ± 0.4 × 10^8$ spores, compared to $2.2 ± 0.7 × 10^5$ spores for AAE2 colonies. Thus, AAE2 had suffered a 500-fold reduction in sporulation compared to AAE1.

Viability of AAE1 and AAE2 spores was determined by plating similar numbers of conidia (~250, 125, or 60 per plate) and counting the number of colonies formed after 2 d incubation at 28 °C. Plates inoculated with ~60 spores each produced 49 AAE1 and 48 AAE2 colonies, with comparable results for the higher inoculation densities, suggesting that spore viability was not compromised by *ugmAΔ*.

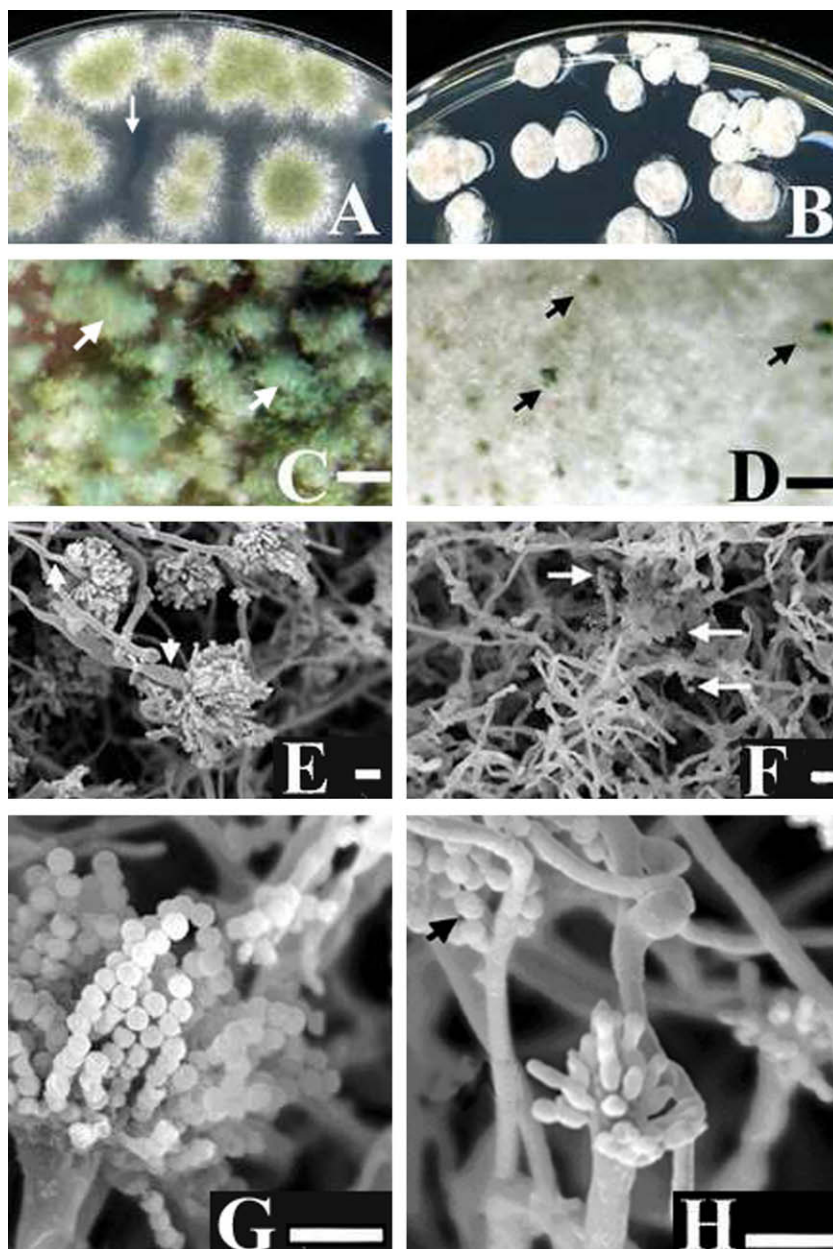


Fig. 3. Conidiation in *Aspergillus nidulans* wildtype AAE1 (A, C, E, and G), and UDG-galactopyranose mutase deletion strain AAE2 (B, D, F, and H), 3 d after inoculation. (A and B) Colony morphology of AAE1 and AAE2 strains. The centres of AAE1 colonies (A) have green conidia, whereas AAE2 colonies (B) have only faint pigmentation due to sparse conidiation. AAE1 colonies are surrounded by a fringe of hyphae extending into the medium (arrows in A) whereas these are lacking in AAE2 colonies. (C and D) A stereomicroscope images of the centres of colonies in A and B. Bars in C and D = 100 μm . As seen from above, an AAE1 colony (C) has closely packed conidial heads, whereas an AAE2 colony (D) has relatively few, widely separated, conidial heads that produced mature green conidia (e.g., arrows). (E–H) Scanning electron micrographs of AAE1 (E and G) and AAE2 colonies (F and H). Bars in E–H = 10 μm . AAE1 colonies (E and G) produce conidiophores (arrowheads) with conidial heads bearing long chains of spores, whereas AAE2 colonies had sterile aerial hyphae with sparse conidiation (arrows in F). (H) An AAE2 colony showing chains of spores (arrow) on one conidial head, whereas others have abnormal or arrested development.

Conidiation in AAE1 and AAE2 was examined using SEM (Fig. 3E–H). By 3 d, AAE1 produced long chains of conidia (Fig. 3E and G), whereas AAE2 colonies (Fig. 3F and H) had relatively few conidiophores (arrows in Fig. 3F) with at most short chains of conidia (s in Fig. 3H), despite abundant sterile hyphae (Fig. 3F). Often, formation of metulae and phialides in AAE2 was arrested or aberrant.

3.3. Hyphal morphology and wall composition

The effect of *ugmA* Δ on hyphal morphogenesis is shown in Fig. 4. Unlike AAE1, which had a wildtype phenotype (Fig. 4 inset),

AAE2 strains stained with Calcofluor Fig. 4A had wide, highly branched hyphae. The AAE2 and AAE1 hyphae in Fig. 4A were stained with the same solution of Calcofluor and Hoechst 33258, and imaged with the same confocal settings. Lateral walls, but few nuclei, were visible in the AAE2 hyphae, whereas the converse was true for AAE1. We interpret this as meaning the AAE2 hyphal walls were relatively thicker than those of AAE1.

AAE1 and three *ugmA* Δ strains including AAE2 were compared by cell morphometry for hyphal width, basal cell length, total hyphal length per germling, and total tips per germling (Table 2A). Relative branching was quantified using the hyphal growth index described by Trinci (1974), as the total hyphal length of a germling

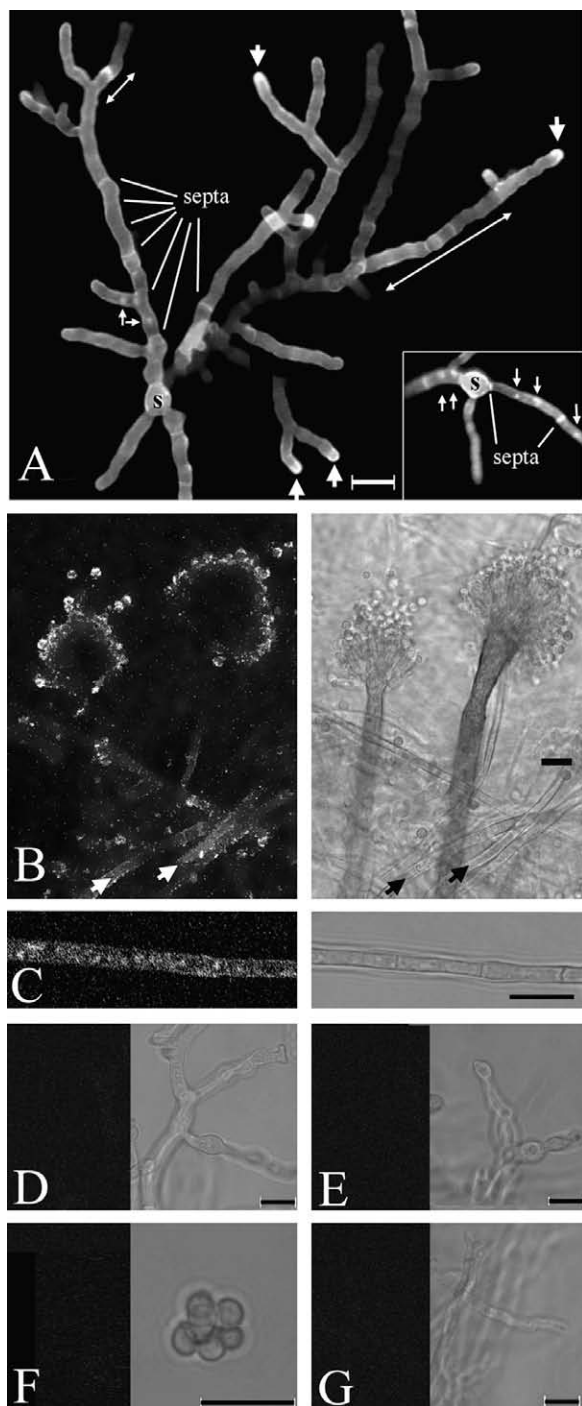


Fig. 4. Walls of *Aspergillus nidulans* AAE2 (*ugmAΔ*) and AAE1 (wildtype) strains following (A) Calcofluor staining at 16 h, or (B–F) Galf immunolocalization at 36 h. Bars = 10 μ m. (A) Germlings were stained with the same solution of Hoechst 33258 for nuclei and Calcofluor for cell walls, and visualized with confocal microscopy. The AAE2 hyphal walls are thick, and stain unevenly: double-headed arrows indicate hyphal walls with considerable variability in staining intensity despite being near-medial optical sections. Some AAE2 hyphal tips stained intensely (large arrows) while other did not, even though both types were a similar optical section. Wildtype morphology AAE1 hyphal walls (A, inset) stained lightly compared to septa and spore (s) walls. Unlike the wildtype strain, hyphal wall staining in the AAE2 strain often obscured visualization of nuclei (small arrows). (B–G) Paired immunofluorescence and transmitted images of Galf localization using the EBA2 monoclonal antibody (see Section 2). (B) In the AAE1 strain, Galf was present in hyphal walls (arrows), in spores, and to a slight extent in phialides. No localization was detected on the conidiophore or metula walls. (C) Galf in hyphal walls of AAE1. The AAE2 conidiophores (D and E), spores (F), and hyphae (G) did not stain under the same preparation and imaging conditions as used for (B) and (C).

divided by the number of tips for that germling. Compared to AAE1, all three *ugmAΔ* strains had more than twofold lower hyphal growth index (Table 2A), indicating at least double the branching frequency.

Galf can be immunolocalized with a monoclonal antibody, EBA2 (Wallis et al., 2001). We used EBA2 to compare Galf content and distribution in AAE1 and AAE2 strains. EBA2 binding in AAE1 Fig. 4B localized to mature conidia and phialides (Fig. 4B), and hyphae (Fig. 4B and C), but not to conidiophores and metulae (Fig. 4B and data not shown). Control AAE1 samples where EBA2 was omitted did not bind the FITC-conjugated secondary antibody. In contrast to AAE1, the spore and hyphal walls of the AAE2 strain did not bind EBA2 (Fig. 4D–G). Thus, AAE2 is depleted for Galf in its walls, consistent with the expected function of the *ugmA* gene product.

Hyphal morphogenesis defects and branching abnormalities in the *ugmAΔ* strains in Table 2A suggested that *ugmA* deletion had impaired fungal wall formation and/or maturation. The growth morphology of AAE2 was assessed on CM containing sucrose and/or Calcofluor (Table 2B). Wildtype morphology strain A28, AAE1, and the three *ugmAΔ* strains for which data are provided in Table 2A were replica-plated on CM with or without sucrose or Calcofluor to assess colony phenotype at 2 d (Fig. 5A–E). Unexpectedly, the colony morphology of A28 and AAE1 strains differed on most media. AAE2 hyphae growing at the edges of the colonies were examined using transmitted light microscopy, directly on the plates to avoid damage from mounting on a microscope slide (Fig. 5F–O). Colonies of AAE1 and the three *ugmAΔ* strains grew differently on these media (Fig. 5A–E), consistent with Fig. 3A and B. Their hyphal morphologies also differed, consistent with Fig. 4A and described quantitatively in Table 2B.

AAE1 hyphae had wildtype morphology when grown on CM (Fig. 5F), whereas AAE2 hyphae had profuse apical branching (Fig. 5K). AAE1 hyphal morphology on CM containing 1 M sucrose was wildtype (Fig. 5G), substantially similar to Fig. 5F, whereas AAE2 grown on 1 M sucrose had a partially remediated hyphal phenotype (Fig. 5L) with reduced but still apical branching. AAE1 hyphae grown on CM containing 10 μ g/mL Calcofluor had a beaded morphology (Fig. 5H), whereas AAE2 hyphae grown on this medium had a partially remediated hyphal phenotype (Fig. 5M), reminiscent of AAE2 growth on 1 M sucrose (Fig. 5L). Like 10 μ g/mL Calcofluor, AAE1 hyphae grown on CM containing 30 μ g/mL Calcofluor had a beaded morphology (Fig. 5I), whereas AAE2 hyphae grown on this medium were highly branched (Fig. 5N). AAE1 hyphae grown on 30 μ g/mL Calcofluor plus 1 M sucrose had a wildtype phenotype (Fig. 5J). Many AAE2 hyphae had a wildtype phenotype this medium, however, bursting was frequent (e.g., arrow in Fig. 5O), despite being examined directly on the Petri plate, suggesting that their walls were fragile.

The effect of growth on CM containing 1 M sucrose or 10 μ g/mL Calcofluor on the *ugmAΔ* strains was quantified morphometrically (Table 2B). AAE1 strains were slightly affected by growth on these media particularly regarding hyphal extension. For the *ugmAΔ* strains, growth on amended medium significantly reduced hyphal width, and had comparable relative effects on growth and branching (shown as hyphal growth index).

3.4. Hyphal wall ultrastructure

Relative hyphal wall thickness was inferred for wildtype AAE1 and *ugmAΔ* strain AAE2 using Calcofluor and Hoechst 33258 dual-stained samples (Fig. 4A). The same dye concentrations and imaging conditions were used for both strains. Lateral walls of AAE2 hyphae (Fig. 4A) stained brightly, but not those of AAE1 (inset). For the AAE2 hyphae, hyphal wall staining obscured visualization of all but a few nuclei (arrows in Fig. 4A), unlike AAE1 hyphae

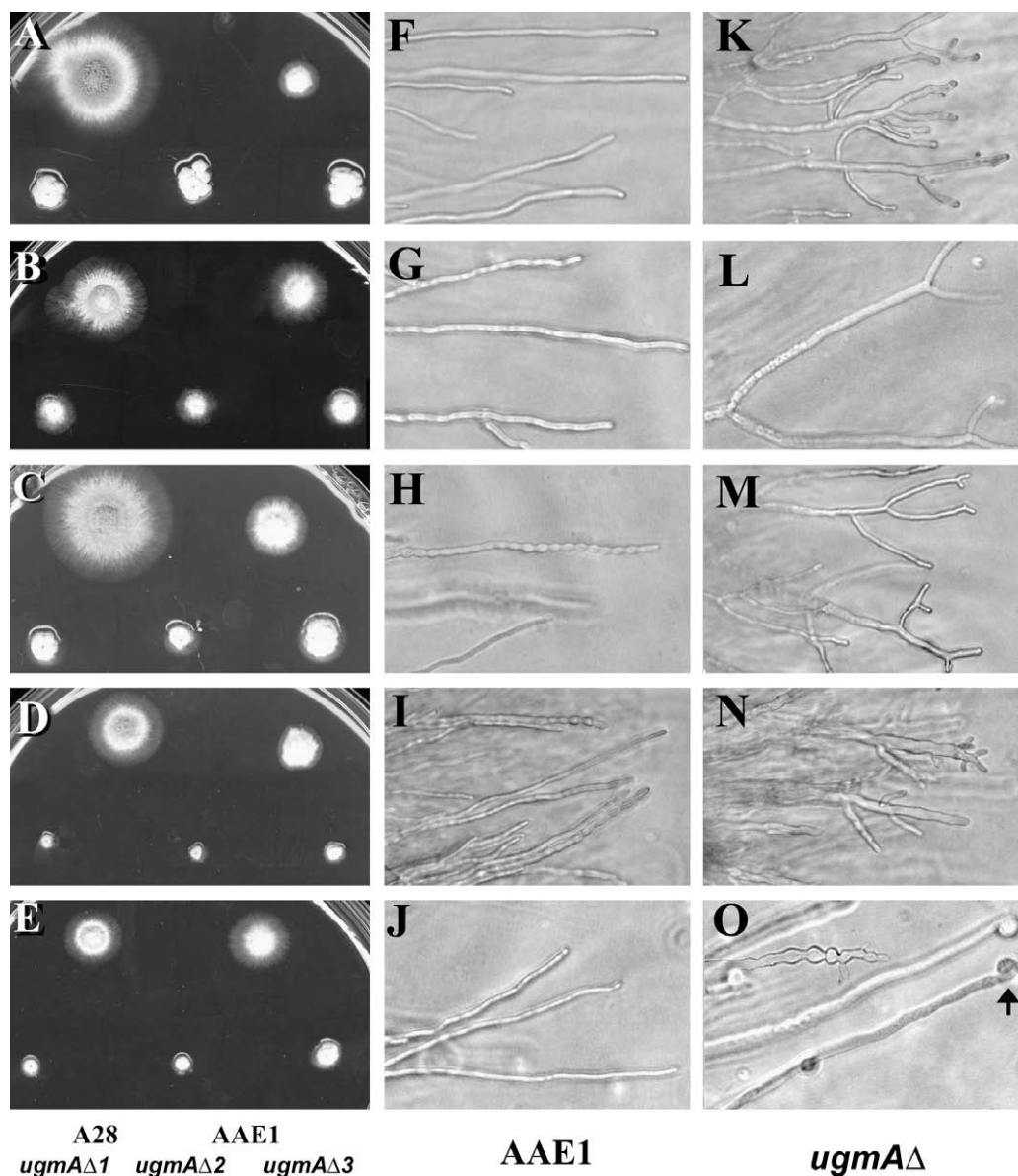


Fig. 5. Colony growth (A–E) and hyphal morphology for AAE1 (F–J) and *ugmAΔ* strains (K–O) after 2 d. Map to the inoculation pattern is at the bottom left. Strains were grown on complete medium, CM (A, F, and K); on CM + 1 M sucrose (B, G, and L); on CM + 10 μ g/mL Calcofluor (C, H, and M); on CM + 30 μ g/mL Calcofluor (D, I, and N); on CM + 1 M sucrose + 30 μ g/mL Calcofluor (E, J, and O).

(arrows in Fig. 4A inset). For both strains, wall staining was evident at septa and in spore walls. We interpret this difference to mean that the lateral walls of the AAE2 hyphae are thicker than those of wildtype.

Transverse TEM sections of AAE1 and AAE2 hyphae (that is, with well resolved cell membrane bi-layers) were used to compare hyphal diameter and wall thickness. Hyphal diameters imaged with TEM (Fig. 6) were consistent with Calcofluor-stained samples imaged with fluorescence microscopy (Fig. 4A and Table 2). Both AAE1 and AAE2 hyphae imaged by TEM had abundant, well-preserved cytoplasmic organelles, suggesting that the hyphae were likely to have been growing at the time of fixation. The AAE2 walls grown on CM (Fig. 6A–D) were significantly thicker than those of AAE1 (Fig. 6E and F), or of AAE2 grown on 1 M sucrose (Fig. 6G and H) or 10 μ g/mL Calcofluor (Fig. 6I and J). Wall thicknesses in transverse TEM sections are shown in Table 2. Walls of AAE2 hyphae grown on CM had distinct layering of moderately electron-dense material, compared to walls of AAE1 hyphae grown on CM,

or walls of AAE2 hyphae grown on 1 M sucrose or 10 μ g/mL Calcofluor (Fig. 6 and Table 2). The AAE2 walls appeared to be similar to wildtype when grown on CM containing 1 M sucrose or 10 μ g/mL Calcofluor.

4. Discussion

The *A. nidulans* genome has a single sequence, AN3112.4, with high homology to UDP-galactopyranose mutase identified in other systems, which we call *ugmA*. Replacing the *ugmA* coding sequence with *AfpyrG* showed that *A. nidulans* *ugmA* is not essential. The *ugmAΔ* strains grew on medium lacking pyrimidines, and could complete their asexual life cycle, producing viable conidia. However, *ugmAΔ* strains had compact colonial growth, reduced conidiation, and aberrant hyphal morphology and wall structure. UGM is not essential in the protozoan *L. major*, but its deletion led to attenuated virulence (Kleczyka et al., 2007). Studies on prokaryotic UGM showed it was essential for growth and viability in bacteria (Pan

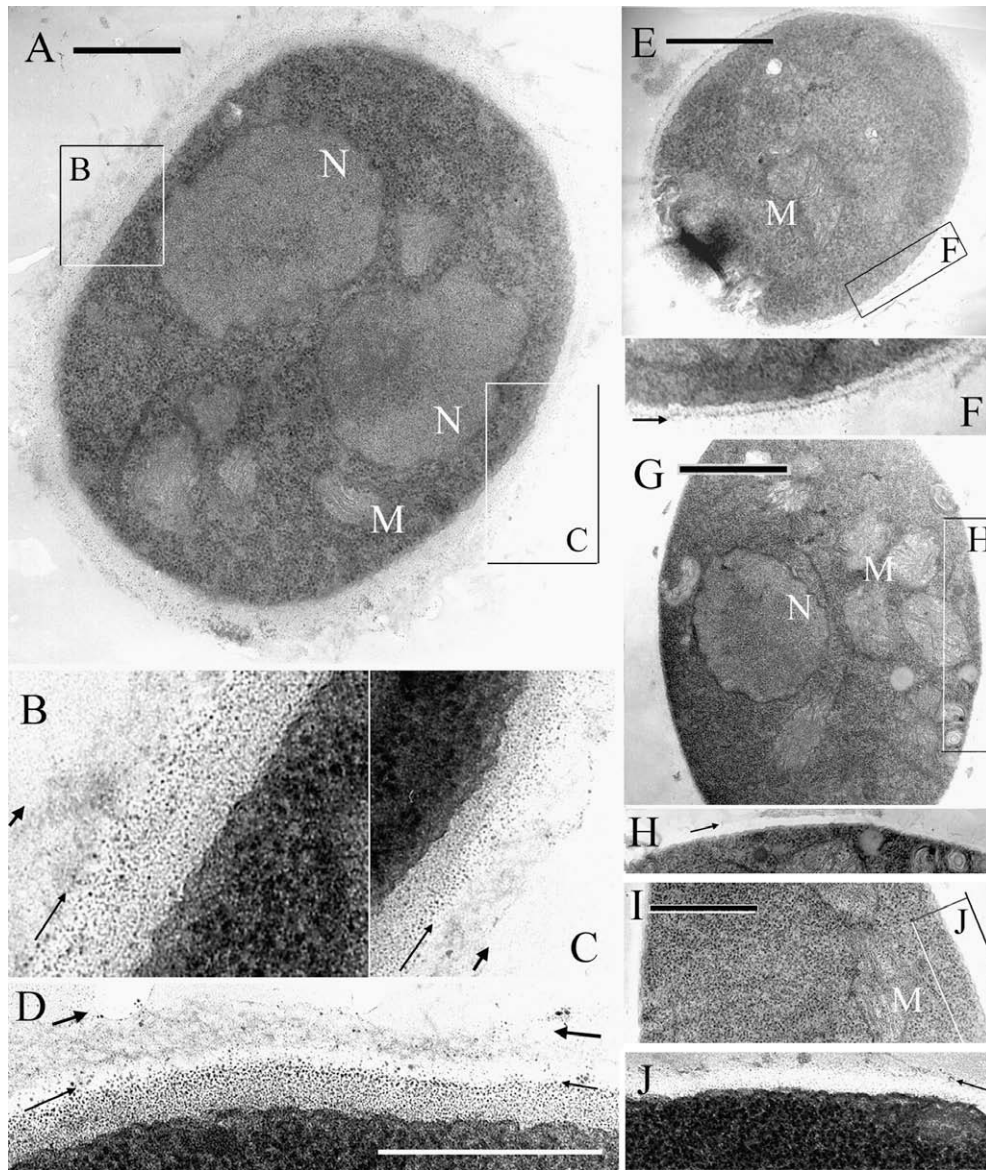


Fig. 6. Transmission electron micrographs of *Aspergillus nidulans* *ugmA* strain AAE2 (A–D) and wildtype strain AAE1 (E–F) growing on complete medium (CM); AAE2 hyphae growing on CM containing 1 molar sucrose (G–H) or CM containing 10 μ g/mL Calcofluor (I–J). Bars in A, E, G, I = 1 μ m. Images in B–C, F, H, J are transverse sections that correspond to the boxed regions in A, E, G, I, respectively, and have been contrast-adjusted and magnified to highlight wall structure. Image D is a transverse section of another AAE2 hypha growing on CM for which a full cross section was not available. Arrows indicate the outer edge of the two prominent wall layers for AAE2 hyphae growing on CM (A–D), and the outer wall of hyphae in other samples (F, H, J). N, nucleus; M, mitochondrion.

et al., 2001). Similarly, *A. fumigatus* *glfA* is not essential, but contributes to pathogenicity when tested in immunosuppressed mice (Schmalhorst et al., 2008).

Galf has been found in *A. nidulans* cell walls (Bennett et al., 1984), consistent with results of Wallis et al. (2001) who used monoclonal antibody EBA2 to immunolocalize *Galf* to conidia and conidiophores in *A. niger*. For strain AAE1, we had strong EBA2 localization to conidia and to a lesser extent to hyphae and phialides. Even with high-sensitivity confocal imaging settings, we had no immunofluorescent signal for AAE2 conidiophores and metulae, although perhaps this could be due to masking from outer wall layers. In contrast to AAE1, none of the AAE2 cell types bound EBA2, suggesting that they were indeed depleted for *Galf*. Thus, the presence of *Galf* in hyphal and conidial walls of *A. nidulans* appears to be due to the action of *ugmA*.

Damveld et al. (2008) screened for cell wall mutants in *A. niger*, using a constitutively activated stress response pathway to seek genes involved in cell wall integrity. They identified mutants in a

UGM homologue, *A. niger* *ugmA*, and showed by sequence comparison that *A. niger* and *A. nidulans* *ugmA* were closely related. Like *A. niger*, *A. nidulans* *ugmA* is predicted to have five introns (Damveld et al., 2008). Related *A. niger* sequences designated *ugmB* were present in at least two other *Aspergillus* spp, but not in *A. nidulans*. The *A. niger* *ugmB* sequence was full length, but *ugmB* Δ in a wild-type or in a *ugmA* Δ background did not generate an additional phenotype (Damveld et al., 2008). Unlike *ugmA*, *ugmB* function is unknown.

Aspergillus niger *ugmA* Δ strains showed increased sensitivity to Calcofluor compared to a wildtype strain (Damveld et al., 2008), consistent with results from Kim et al. (2008). Unexpectedly, the *A. nidulans* AAE2 hyphal phenotype was partially remediated on medium containing 10 μ g/mL (but not 30 μ g/mL) Calcofluor; this phenotype was reminiscent of growth on 1 M sucrose. This result is consistent with our TEM results showing that AAE2 cell wall thickness on CM containing 10 μ g/mL Calcofluor was about a third as thick as on CM alone. *Aspergillus nidulans* mutants that are

hypersensitive to growth on Calcofluor have been described previously (Hill et al., 2006), as has remediation on high osmolarity medium, but to our knowledge Calcofluor remediation has not. Damveld et al. (2008) assessed colony growth of *A. niger* *ugmA* mutants on medium containing 10 µg/mL Calcofluor, but did not examine them microscopically. Calcofluor treatment has been shown to increase chitin production in *Saccharomyces* (García-Rodríguez et al., 2000) but apparently that chitin is weaker, so the mechanism by which remediation occurs is unclear.

The *ugmA* deletion had a dramatic effect on *A. nidulans* hyphal walls imaged with TEM, and wall thicknesses measured with TEM were consistent with relative Calcofluor staining. Damveld et al (2008, and references therein) suggest that wall stress may induce compensatory synthesis of chitin and α -glucan. A comparable effect could account for the increased wall thickness in our AAE2 hyphal walls and changes in Calcofluor binding. Following partial remediation by growing AAE2 on 1 M sucrose or 10 µg/mL Calcofluor, hyphal wall cross-sections imaged by TEM resembled those of AAE1. Thus, at least some of the defects induced by deletion of *A. nidulans* *ugmA* can be remediated by treatments likely to have substantially different targets.

In contrast to our TEM results showing that AAE1 walls were significantly thinner than those of AAE2, Schmalhorst et al. (2008) found using freeze fracture SEM that wildtype *A. fumigatus* hyphal walls were substantially thicker than those of a Δ *glfA* strain. The *A. fumigatus* hyphae may have been older than ours (which were 16 h), since they lacked substantial cytoplasm. In addition, TEM and SEM preparation techniques differ substantially. If the Δ *glfA* wall were as diffuse as that of AAE2 hyphae, it could have collapsed during drying. Given that walls of the wildtype *A. fumigatus* (Schmalhorst et al., 2008) and *A. nidulans* (this study) strains had substantially different thickness, even though they have similar overall composition (Guest and Momany, 2000), it will be important in the future to compare similar aged cells with both techniques.

In sum, we have shown that *A. nidulans* *ugmA* is important for wildtype growth, but is not essential for survival. The *ugmA* Δ phenotype is consistent with defects related in cell wall deposition and maturation. We are continuing to explore the biochemistry and ultrastructure of *A. nidulans* *ugmA* Δ strains.

Acknowledgments

This research was supported by Natural Science and Engineering Research Council of Canada Discovery grants and a Canadian Institutes of Health Research/Regional Partnership Program grant to SGWK and DARS, and by an Egyptian Ministry of Higher Education grant to A.M.E. We thank Tom Bonli (Department of Geological Sciences, University of Saskatchewan) for assistance with the scanning electron microscope (SEM), Dr. Robbert Damveld for providing a copy of their accepted manuscript prior to publication, and anonymous Reviewers for suggestions.

Appendix A. Supplementary data

Supplementary data associated with this article can be found, in the online version, at doi:10.1016/j.fgb.2008.09.008.

References

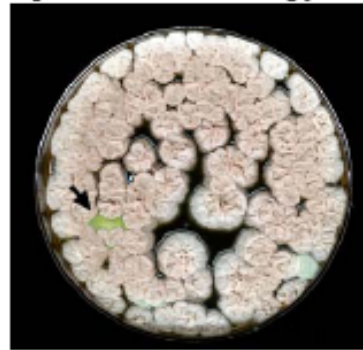
Adams, T.H., Wieser, J.K., Yu, J.-H., 1998. Asexual sporulation in *Aspergillus nidulans*. *Microbiol. Mol. Biol. Rev.* 62, 35–54.
 Arathoon, E.G., 2001. Clinical efficacy of echinocandin antifungals. *Curr. Opin. Infect. Dis.* 14, 685–691.
 Bakker, H., Kleczka, B., Gerardy-Schahn, R., Routier, F.H., 2005. Identification and partial characterization of two eukaryotic UDP-galactopyranose mutases. *Biol. Chem.* 386, 657–661.

Bennett, J.E., Bhattacharjee, A.K., Glaudemans, C.P.J., 1984. Galactofuranosyl groups are immunodominant in *Aspergillus fumigatus* galactomannan. *Mol. Immunol.* 22, 251–254.
 Beverly, S.M., Owens, K.L., Showalter, M., Griffith, C.L., Doering, T.L., Jones, V.C., McNeil, M.R., 2005. Eukaryotic UDP-galactopyranose mutase (*GLF* gene) in microbial and metazoal pathogens. *Eukaryot. Cell.* 4, 1147–1154.
 Carrillo-Munoz, A.J., Giusiano, G., Ezkurra, P.A., Quindos, G., 2006. Antifungal agents: mode of action in yeast cells. *Rev. Esp. Quimioterap.* 19, 130–139.
 Chamilos, G., Kontoyiannis, D.P., 2005. Update on antifungal resistance mechanisms of *Aspergillus fumigatus*. *Drug Resist. Updat.* 8, 344–358.
 Costachel, C., Coddeville, B., Latge, J.-P., Fontaine, T., 2005. Glycosylphosphatidylinositol-anchored fungal polysaccharide in *Aspergillus fumigatus*. *J. Biol. Chem.* 280, 39835–39842.
 Cowen, L., 2008. The evolution of fungal drug resistance: modulating the trajectory from genotype to phenotype. *Nat. Rev. Micro.* 6, 187–198.
 Damveld, R.A., Franken, A., Arentshorst, M., Punt, P.J., Klis, F.M., van den Hondel, C.A.M.J.J., Ram, A.F.J., 2008. A novel screening method for cell wall mutants in *Aspergillus niger* identifies UDP-galactopyranose mutase as an important protein in fungal cell wall biosynthesis. *Genetics* 178, 873–881.
 García-Rodríguez, L., Durán, A., Roncero, C., 2000. Calcofluor antifungal action depends on chitin and a functional high-osmolarity glycerol response (HOG) pathway: evidence for a physiological role of the *Saccharomyces cerevisiae* HOG pathway under non-inducing conditions. *J. Bacteriol.* 182, 2428–2437.
 García-Ruiz, J.C., Amutio, E., Pontón, J., 2004. Invasive fungal infection in immunocompromised patients. *Rev. Iberoam. Micol.* 21, 55–62.
 Guest, G.M., Momany, M., 2000. Analysis of cell wall sugars in the pathogen *Aspergillus fumigatus* and the saprophyte *Aspergillus nidulans*. *Mycologia* 92, 1047–1050.
 Hill, T.W., Loprete, D.M., Momany, M., Harsch, M., Livesay, J.A., Mirchandani, A., Murdock, J.J., Vaughan, M.J., Watt, M.B., 2006. Isolation of cell wall mutants in *Aspergillus nidulans* by screening for hypersensitivity to Calcofluor White. *Mycologia* 98, 399–409.
 Kaminskyj, S.G.W., 2000. Septum position is marked at the tip of *Aspergillus nidulans* hyphae. *Fungal. Genet. Biol.* 31, 105–113.
 Kaminskyj, S.G.W., 2001. Fundamentals of growth, storage, genetics and microscopy of *Aspergillus nidulans*. *Fungal. Genet. News.* 48, 25–31.
 Kaminskyj, S.G.W., Hamer, J.E., 1998. *Hyp* loci control cell pattern formation in the vegetative mycelium of *Aspergillus nidulans*. *Genetics* 148, 669–680.
 Kaminskyj, S.G.W., Heath, I.B., 1995. Integrin and spectrin homologues, and cytoplasm-wall adhesion in tip growth. *J. Cell Sci.* 108, 849–856.
 Kim, J., Campbell, B., Mahoney, N., Chan, K., Molyneux, R., May, G., 2008. Chemosenitization prevents tolerance of *Aspergillus fumigatus* to antimycotic drugs. *Biochem. Biophys. Res. Commun.* 372, 266–271.
 Kleczka, B., Lamerz, A.-C., Zandbergen, G., Wenzel, A., Gerardy-Schahn, R., Wiese, M., Routier, F.H., 2007. Targeted gene deletion of *Leishmania major* UDP-galactopyranose mutase leads to attenuated virulence. *J. Biol. Chem.* 282, 10498–10505.
 Koplin, R., Brisson, J.R., Whitfield, C., 1997. UDP-galactofuranose precursor required for formation of lipopolysaccharide O antigen of *Klebsiella pneumoniae* serotype O1 is synthesized by the product of the *rj**BD*_{KP01} gene. *J. Biol. Chem.* 272, 4121–4128.
 Latgé, J.-P., Kobayashi, H., Debeaupuis, J.-P., Diaquin, M., Sarfati, J., Wieruszkeski, J.-M., Parra, E., Bouchara, J.-P., Fournet, B., 1994. Chemical and immunological characterization of the extracellular galactomannan of *Aspergillus fumigatus*. *Infect. Immun.* 62, 5424–5433.
 Leitao, E.A., Bitte, V.C.B., Haido, R.M.T., Valente, A.P., Peter-Katalinic, J., Letzel, M., de Souza, L.M., Barreto-Bergter, E., 2003. β -Galactofuranose-containing O-linked oligosaccharides present in the cell wall peptidogalactomannan of *Aspergillus fumigatus* contain immunodominant epitopes. *Glycobiology* 13, 681–692.
 Loffler, J., Stevens, D.A., 2003. Antifungal drug resistance. *CID* 36 (Suppl. 1), S31–S41.
 Maertens, J., Theunissen, K., Lodewyck, T., Lagrou, K., Eldere, J., 2007. Advances in the serological diagnosis of invasive *Aspergillus* infections in patients with haematological disorders. *Mycoses* 50 (Suppl. 1), 2–17.
 Nassau, P.M., Martin, S.L., Brown, R.E., Weston, A., Monsey, D., McNeil, M.R., Duncan, K., 1996. Galactofuranose biosynthesis in *Escherichia coli* K-12: identification and cloning of UDP-galactopyranose mutase. *J. Bacteriol.* 178, 1047–1052.
 Nayak, T., Szewczyk, E., Oakley, C.E., Osmani, A., Ukil, L., Murray, S.L., Hynes, M.J., Osmani, S.A., Oakley, B.R., 2006. A versatile and efficient gene-targeting system in *Aspergillus nidulans*. *Genetics* 172, 1557–1566.
 Notermans, S., Veeneman, G.H., van Zuylen, C.W.E.M., Hoogerhout, P., van Boom, J.H., 1998. (1 \rightarrow 5)-linked β -D-galactofuranosides are immunodominant in extracellular polysaccharides of *Penicillium* and *Aspergillus* species. *Mol. Immunol.* 25, 975–979.
 Osmani, A.H., Oakley, B.R., Osmani, S.A., 2006. Identification and analysis of essential *Aspergillus nidulans* genes using the heterokaryon rescue technique. *Nat. Protoc.* 1, 2517–2526.
 Pan, F., Jackson, M., Ma, Y., McNeil, M., 2001. Cell wall core galactofuran is essential for growth of *Mycobacterium*. *J. Bacteriol.* 183, 3991–3998.
 Pederson, L.L., Turco, S.J., 2003. Galactofuranose metabolism: a potential target for antimicrobial chemotherapy. *Cell. Mol. Life Sci.* 60, 259–266.
 Randhawa, G.K., Sharma, G., 2004. Echinocandins: a promising new antifungal group. *Indian J. Pharmacol.* 36, 65–71.
 Sanders, D.A.R., Staines, A.G., McMahon, S.A., McNeil, M.R., Whitfield, C., Naismith, J.H., 2001. UDP-galactopyranose mutase has a novel structure and mechanism. *Nat. Struct. Biol.* 8, 858–863.

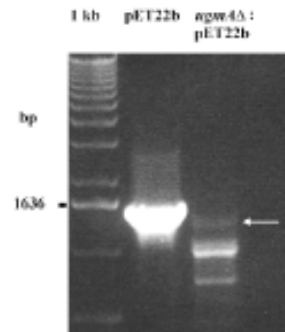
- Schmalhorst, P.S., Krappmann, S., Vervecken, S.W., Rohde, M., Müller, M., Braus, G.H., Contreras, R., Braun, A., Bakker, H., Routier, F.H., 2008. Contribution of galactofuranose to the virulence of the opportunistic pathogen *Aspergillus fumigatus*. *Eukaryot. Cell* 7, 1268–1277.
- Shaw, B.D., Momany, M.M., 2002. *Aspergillus nidulans* polarity mutant *swaA* is complemented by protein O-mannosyltransferase *pmtA*. *Fungal. Genet. Biol.* 37, 263–270.
- Shi, X., Sha, Y., Kaminskyj, S., 2004. *Aspergillus nidulans hypA* regulates morphogenesis through the secretion pathway. *Fungal. Genet. Biol.* 41, 75–88.
- Spath, G.F., Epstein, L., Leader, B., Singer, S.M., Avila, H.A., Turco, S.J., Beverley, S.M., 2000. Lipophosphoglycan is a virulence factor distinct from related glycoconjugates in the protozoan parasite *Leishmania major*. *Proc. Natl. Acad. Sci. USA* 97, 9258–9263.
- Stevenson, G.G., Andrianopoulos, K., Hobbs, M., Reeves, P.R., 1996. Organization of the *Escherichia coli* K-12 gene cluster responsible for production of the extracellular polysaccharide colonic acid. *J. Bacteriol.* 178, 4885–4893.
- Stynen, D., Sarafati, J., Goris, A., Prevost, M.-C., Lesourd, M., Kamphuis, H., Darras, V., Latgé, J.-P., 1992. Rat monoclonal antibodies against *Aspergillus* galactomannan. *Infect. Immun.* 60, 2237–2245.
- Szewczyk, E., Nayak, T., Oakley, C.E., Edgerton, H., Xiong, Y., Taheri-Talesh, N., Osmani, S.A., Oakley, B.R., 2007. Fusion PCR and gene targeting in *Aspergillus nidulans*. *Nat. Protoc.* 1, 3111–3120.
- Tawara, S., Ikeda, F., Maki, K., Morishita, Y., Otomo, K., Teratani, N., Goto, T., Tomishima, M., Ohki, H., Yamada, A., Kawabata, K., Takasugi, H., Sakane, K., Tanaka, H., Matsumoto, F., Kuwahara, S., 2000. *In vitro* activities of a new lipopeptide antifungal agent, FK463, against a variety of clinically important fungi. *Antimicrob. Agents Chemother.* 44, 57–62.
- Trinci, A.P.J., 1974. A study of the kinetics of hyphal extension and branch initiation of fungal mycelia. *J. Gen. Microbiol.* 81, 225–236.
- Wallis, G.L.F., Hemming, F.W., Peberdy, J.F., 2001. β -Galactofuranoside glycoconjugate on the conidia and conidiophores of *Aspergillus niger*. *FEMS Microbiol. Lett.* 201, 21–27.
- Weston, A., Stern, R.J., Lee, R.E., Nassau, P.M., Monsey, D., Martin, S.L., Scherman, M.S., Besra, G.S., Duncan, K., McNeil, M.R., 1998. Biosynthetic origin of mycobacterial cell wall galactopyranosyl residues. *Tuberc. Lung Dis.* 78, 123–131.
- Whitfield, C., Richards, J.C., Perry, M.B., Clarke, B.R., Maclean, L.L., 1991. Expression of two structurally distinct β -galactan O antigens in the lipopolysaccharide of *Klebsiella pneumoniae* serotype O1. *J. Bacteriol.* 173, 1420–1431.
- Yang, Y., El-Ganiny, A.M., Bray, G.E., Sanders, D.A.R., Kaminskyj, S.G.W., 2008. *Aspergillus nidulans hypB* encodes a Sec7-domain protein important for hyphal morphogenesis. *Fungal. Genet. Biol.* 45, 749–759.

Supplemental Figure 1 – Rescue of the *ugmAΔ* phenotype by complementation with *AfglfA*

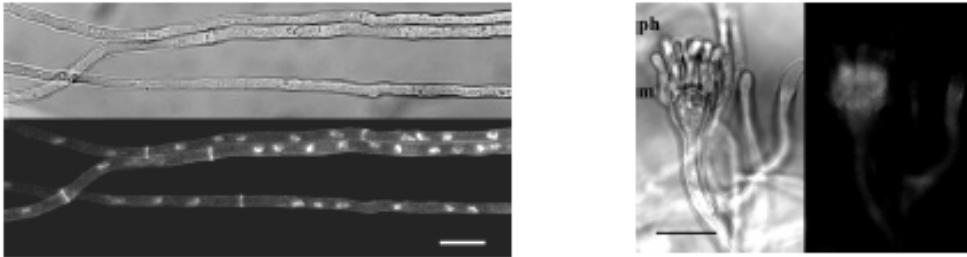
a) AAE2 (*ugmAΔ*) colonies transformed with *AfglfA* protein expression plasmid pET22b. *AfglfA* from pET22b has been shown to mediate Gal β -Gal α conversion (Bakker *et al.* 2005 Biol Chem. 386, 657-662). After 4 d growth at 37 °C, a single putative *ugmAΔ*:*AfglfA* colony with wildtype green conidia (black arrow) amongst many *ugmAΔ* colonies.



b) PCR of pET22b and of genomic DNA template extracted from the putative *ugmAΔ*:*AfglfA* colony shown in (a) using primers *AfglfAF* [CCCTCCAGCTCCGTCGAC] and *AfglfAR* [CTGGCCTTGCTCTTGGC]. We believe that pET22b has integrated into the genome, since in six independent experiments we have been unable to rescue pET22b by transforming genomic DNA extracted from this strain into *E. coli* and selecting for ampicillin resistance. Differences in template concentration are consistent with the weak amplification of *AfglfA* from genomic DNA.



c) Hyphae (left) and a typical young conidiophore (right) of the *ugmAΔ*:*AfglfA* strain, which were stained with Calcofluor for septa and Hoechst 33258 for nuclei, and imaged with confocal epifluorescence microscopy. Nuclear morphology and spacing in the hyphae (left) is consistent with wildtype strains. Note synchronous development of metulae (m) and phialides (ph). Bars = 10 μ m.

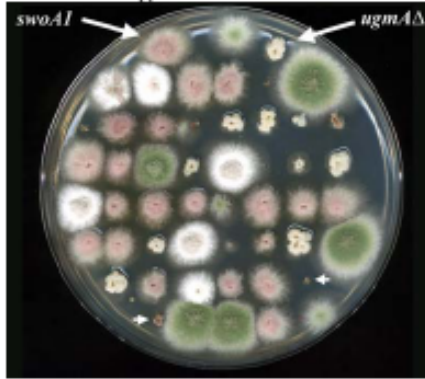


d) Morphometry of the *ugmAΔ*:*AfglfA* strain hyphae. Width: $3.0 \pm 0.1 \mu$ m (n=50); basal cell length: $39.9 \pm 2.9 \mu$ m (n=30). Compare with *ugmAΔ* strains (Table 2).

Supplemental Figure 2: Following mating, *ugmA* segregates independently of *nkuA* and *swoA*.

AAE2 (*ugmA::AfpyrG*; *nkuA::argB*; *pyroA1*) and AOZ1 (*swoA1^{tr}*; *wA3*; *argB2*; GFP-*tubA*) were mated as described in Kaminskyj (2001). AOZ1 was created by mating *swoA1* strain AXL4 (a gift of Michelle Momany: Shaw and Momany 2002 Fung. Genet. Biol. 37: 263-270) and LO1022 (a gift of Liz and Berl Oakley: Horio and Oakley 2005 Molec. Biol. Cell 16: 918-926). Cleistothecia from the AAE2::AOZ1 cross containing viable spores were isolated only following extended incubation, ~3 months.

a) Independent inheritance of *ugmAΔ* and *swoA1*. Typical results are shown for single ascospore progeny from an AAE2::AOZ1 cross. Parental *swoA1* and *ugmAΔ* strains and their progeny were grown on fully supplemented medium at 37 °C. Both *ugmAΔ* and *swoA1* have diminished sporulation at 37 °C, but can be distinguished by their colony morphologies. Wildtype vs diminished sporulation was seen in 43 : 97 progeny, which is consistent with independent segregation of *ugmAΔ* and *swoA1*, and severely defective growth of [*ugmAΔ*, *swoA1*] double mutants (e. g., arrowheads). For all single ascospore colonies showing wildtype sporulation, green : white = 22 : 21. Together, these data are consistent with independent inheritance of *ugmAΔ* and *swoA1*.



b) Independent inheritance of *ugmA* and *nkuA* in progeny from AAE2::AOZ1. Genomic DNA was extracted from six randomly-selected progeny with the *ugmAΔ* colony phenotype, and tested for the presence of *nkuA⁺* using PCR and primers *nkuAF* [CCCCGTCCGTCTGCAG], and *nkuAR* [AACTTCGTCTCAAGTAACTCCTCCAC], which are expected to amplify a 1981 bp fragment. Segregation of *nkuAΔ* and *nkuA⁺* (lanes ABC and DEF, respectively), independent of *ugmA*. The positive control template was *A. nidulans* A28 genomic DNA (lane G).

